Tellus (2007), 59A, 562–569
Printed in Singapore.

TELLUS

The relative vorticity of ocean surface winds from the QuikSCAT satellite and its effects on the geneses of tropical cyclones in the South China Sea

By LEI WANG[1]*, KAI-HON LAU[2,3], CHI-HUNG FUNG[1] and JIAN-PING GAN[1,3], [1]*Department of Mathematics, Hong Kong University of Science and Technology, Hong Kong, China;* [2]*Institute for the Environment, Hong Kong University of Science and Technology, Hong Kong, China;* [3]*Atmospheric, Marine and Coastal Environment Program, Hong Kong University of Science and Technology, Hong Kong, China*

(Manuscript received 5 December 2006; in final form 22 March 2007)

ABSTRACT

This study finds a relationship between the distribution of the seven-year mean relative vorticity of surface winds (RVSW) derived from 25-kilometer-resolution measurements of ocean winds from the Quick Scatterometer (QuikSCAT) satellite and the genesis locations of tropical cyclones (TCs) in the South China Sea (SCS). The results show the effects of the background mean RVSW on TC formation in the SCS. During the summer monsoon, TCs are formed in the northern SCS, where monsoon trough and coastal mountains contribute to positive mean RVSW, while during the winter monsoon TCs form in the southern SCS with positive mean RVSW. No TCs formed in the southern part of the SCS during the summer monsoon nor in the northern part during the winter monsoon during the period from 1945 to 2005, both of which coincide with negative mean RVSW induced by the coastal mountains. The mean RVSW prior to TC formation in regions around the TC genesis locations are calculated using the QuikSCAT measurements averaged over 3 d before the geneses of 36 TCs formed in the SCS from July 1999 to June 2006. The value of this mean RVSW in the SCS is 6.19×10^{-5} s^{-1}, which is about 1.7 times the planetary vorticity at the TC genesis positions and about 5.0 times the seven-year monthly mean RVSW. The results of these quantitative calculations using the direct satellite observations support the hypothesis given by Gray in 1975 that above-normal low-level relative vorticity is necessary for the occurrence of tropical cyclogenesis.

1. Introduction

Tropical cyclones (TCs) are among the most destructive natural phenomena on the earth, causing serious ecological and human damage. The South China Sea (SCS), a large semi-enclosed marginal sea in the western Pacific Ocean, is one region where TCs occur frequently, and about 13.2% of the TCs in the western North Pacific (WNP), the region of most frequent TC formation on the earth, originate from the SCS (Chen and Ding, 1979; Wang and Fei, 1987). Earlier researchers often counted SCS TCs as WNP TCs (Chen et al., 1998; Chia and Ropelewski, 2002). However, SCS TCs have different characteristics compared with WNP TCs due to the different climatic features of two regions (Zhang, 2003). Compared with TCs in other regions, there is relatively little work in the literature on TC genesis and development in the SCS (Zhang and Lin, 2001; Lau et al., 2003; Wu et al., 2005; Wang et al., 2007).

In the first global climatology of tropical cyclogenesis, Gray (1968) established six environmental conditions (based on three thermodynamic and three dynamic variables) as favourable conditions for the formation of TCs, one of which is large values of low-level relative vorticity. While the necessary thermodynamic conditions exist over a considerable portion of the tropical oceans for long periods of time, the low-level relative vorticity and vertical shear parameters can change significantly on much smaller time and space scales (Gray, 1975; McBride, 1981). Thus, it has been hypothesized that tropical cyclogenesis occurs when above-normal low-level relative vorticity and locally weak vertical wind shear occur within a thermodynamically favourable environment (Gray, 1975).

The low-level relative vorticity over ocean was obtained mainly from objectively analysed data sources with coarse resolution (e.g. European Centre for Medium-Range Weather Forecasts (ECMWF) analysis, 2.5° × 2.5°) previously because of the paucity of direct observations over vast areas of the global ocean. Since July 1999, the Quick Scatterometer (QuikSCAT) has provided spatially extensive wind measurements over the global ocean with high resolution (0.25° × 0.25°), which have revealed

*Corresponding author.
e-mail: leiwang@ust.hk
DOI: 10.1111/j.1600-0870.2007.00249.x

many new features of ocean winds (Chelton et al., 2004). In addition, QuikSCAT satellite wind measurements have been used as a new tool to identify systems that have the potential to develop into TCs (Katsaros et al., 2001; Sharp et al., 2002).

In this study, we obtain the seven-year mean relative vorticity of surface winds (RVSW) in the SCS using the 25-kilometer-resolution measurements of ocean winds from the QuikSCAT satellite. An interesting relationship between the seven-year mean RVSW and genesis locations of TCs in the SCS during summer and winter monsoons is revealed, which shows the effects of the background mean RVSW due to the monsoon trough and coastal mountains on TC formation in the SCS. The three-day mean RVSW prior to TC genesis in 36 individual cyclogenesis events in the SCS from July 1999 to June 2006 is also calculated to indicate the character of the RVSW induced by synoptic-scale waves/disturbances prior to TC formation.

This paper is organized as follows. Section 2 describes the data sets and the analysis procedures. Section 3 presents the effects of background mean RVSW on TC formation in the SCS. Section 4 investigates the mean RVSW over the 3 d prior to TC genesis in 36 individual cyclogenesis events in the SCS and section 5 is a summary.

2. Data and methodology

The Sea Winds scatterometer on the QuikSCAT satellite is a microwave radar launched and operated by the U.S. National Aeronautics and Space Administration (NASA). Since July 1999, the QuikSCAT satellite scatterometer has provided spatially extensive measurements of near-surface wind speeds and directions over the world's ocean. With a 1800-km swath, QuikSCAT samples more than 90% of the global ocean every 24 hours. We use the wind speed and direction at a given location obtained from the radar backscatter measurements of sea surface roughness at 25 km resolution and multiple azimuth looks. Comparisons with National Data Buoy Center ocean buoys show that scatterometer wind retrievals are accurate to within 2 m s^{-1} for wind speed and 20° for wind direction measurements, which is essentially equivalent to the accuracy of *in situ* point measurements from buoys (Freilich and Dunbar, 1999). A significant problem affecting scatterometers is rain, which can have a substantial influence on QuikSCAT observations (Bliven et al., 1993; Sobieski et al., 1999). This is, however, a well-documented problem and research (Weissman et al., 2002) has shown that rain is not a fundamental problem for the wind speeds we are studying (i.e. 10–20 m s^{-1}), excluding the effects of intense rains typical at the core of mature TCs.

The mean RVSW in the SCS was calculated using all available QuikSCAT satellite data from July 1999 to June 2006 (i.e. the rain-flagged data were not removed). The inclusion of rain-flagged data likely modifies the vorticity calculations; however, the noise induced by including these data is small compared to the signal. The RVSW at one point ($\zeta_{i,j}$) can be calculated according to eq. (1).

$$\zeta_{i,j} = \left(\frac{\partial v}{\partial x} - \frac{\partial u}{\partial y}\right)_{i,j} = \frac{1}{2d}\left(v_{i+1,j} - v_{i-1,j} - u_{i,j+1} + u_{i,j-1}\right), \quad (1)$$

Where *i* and *j* are indexes of QuikSCAT measurement grid points along the west-east and south-north directions, *u* and *v* are two components of wind along the west-east and south-north directions, and *d* is the spatial distance between two adjacent QuikSCAT measurement points.

The historical record of TC activity in the SCS from 1945 to 2005 was obtained from the best-track archives of the Joint Typhoon Warning Center (JTWC). Each Annual Tropical Cyclone Report issued by the JTWC contains a summary of the best-track positions for all storms for which the JTWC issued a warning during that calendar year. The best-track archives contain six-hourly TC positions and intensity estimates starting from 1945. These TC positions are determined well after each TC has dissipated. Post-storm analysts generally have more raw data, more time and a complete storm history to produce best-track positions for the JTWC Archives. Genesis locations of TCs are defined as the first position on record for a particular TC that attains tropical depression (TD) strength and genesis times of each TC are defined as the first time on record for a particular TC. In the JTWC data set, a TD is defined as a TC with a maximum sustained (1-minute mean) surface wind less than 18 m s^{-1}.

3. The mean RVSW and genesis locations of TCs during summer and winter monsoons

The SCS experiences two monsoons, winter and summer, every year (Wyrtki, 1961; Liang, 1991). During the summer monsoon season, a southwest wind blows over the SCS (Fig. 1a). A typical summer monsoon pattern lasts nearly 4 months (around mid-May to mid-September). During the winter monsoon season, a northeast wind blows over the SCS (Fig. 1b) as a result of the Siberian high pressure system located over the East Asian continent. A typical winter monsoon pattern lasts nearly 6 months (around mid-October to mid-April). Previous statistical studies show that about 97.8% of the TCs form from May to December in the SCS (Wang et al., 2007). In this study, we choose May to September as summer monsoon months and October to December as winter monsoon months. Totally, 160 TCs that formed during the summer monsoon and 65 TCs that formed during the winter monsoon in the SCS throughout the period from 1945 to 2005 are investigated in this study.

The mean RVSW from seven-year QuikSCAT satellite data (from July 1999 to June 2006) and genesis locations of TCs from 61-year JTWC best-track archives (from 1945 to 2005) during summer and winter monsoons are shown in Fig. 2. An apparent relationship between the mean RVSW and the genesis locations of TCs can be seen. In the summer monsoon, TCs are formed in the northern part of the SCS with positive mean

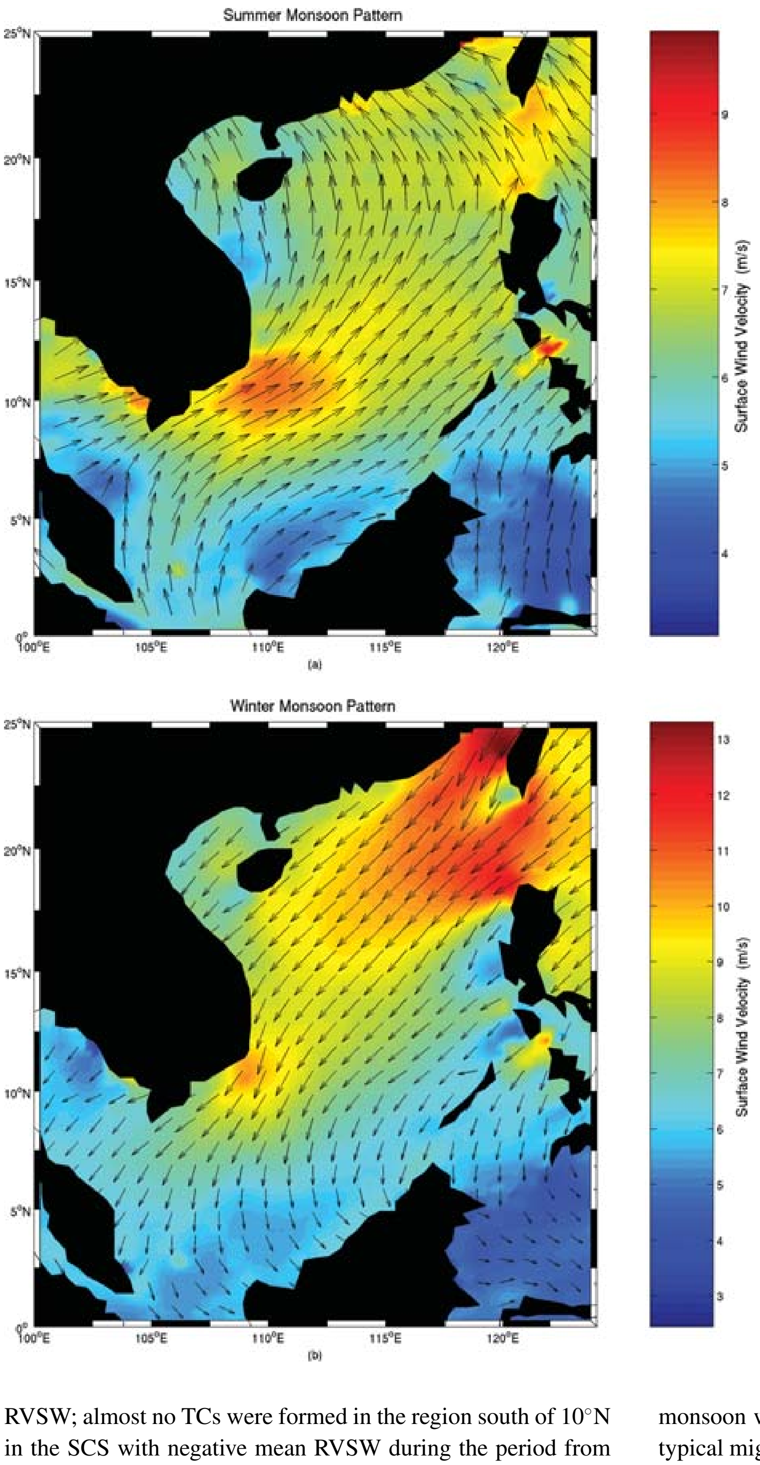

Fig. 1. The mean surface wind vectors and wind velocity (shown by colour) in the SCS for (a) the summer monsoon and (b) the winter monsoon. The mean surface wind is derived from seven-year QuikSCAT satellite data (from July 1999 to June 2006). We choose May to September as the summer monsoon months, and October to December as the winter monsoon months.

RVSW; almost no TCs were formed in the region south of 10°N in the SCS with negative mean RVSW during the period from 1945 to 2005. The winter monsoon pattern is 180 ° out-of-phase with the summer monsoon pattern. The genesis locations of TCs shift to the southern part of the SCS with positive mean RVSW; correspondingly no TCs were formed in the northernmost region of the SCS with negative mean RVSW.

One reason for the positive mean RVSW in the SCS is the monsoon trough. The monsoon trough is the shearline separating the monsoon westerlies from the trade easterlies. Fig. 3 shows the typical migration of the axis of the monsoon trough by its mean monthly position derived from the seven-year mean wind field of QuikSCAT measurements (from July 1999 to June 2006) by determining the interface of the monsoon westerlies and the trade easterlies. The monsoon trough provides the environment with a high positive RVSW (Fig. 4). From June to September, the monsoon trough is typically located in the northern part of the SCS, which is consistent with the positive mean RVSW derived from

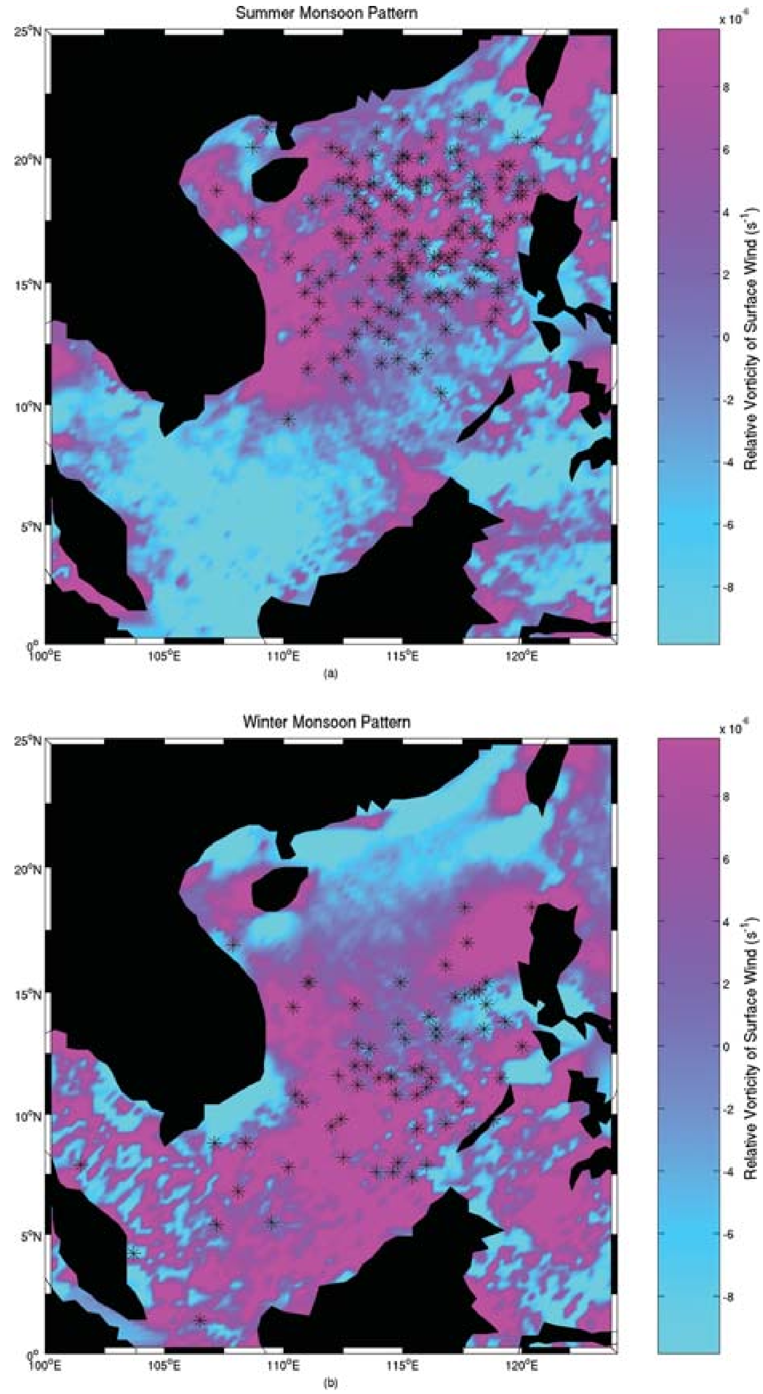

Fig. 2. The mean RVSW (shown by colour) and the genesis locations (indicated by asterisks) of TCs (during the period from 1945 to 2005) in the SCS for (a) the summer monsoon and (b) the winter monsoon. The mean RVSW is derived from seven-year QuikSCAT satellite data (from July 1999 to June 2006). The genesis locations of TCs are obtained from 61-yr best-track archives (during the period from 1945 to 2005). Totally genesis locations of 160 TCs during the summer monsoon and 65 TCs during the winter monsoon are plotted. We choose May to September as the summer monsoon months, and October to December as the winter monsoon months.

the seven-year QuikSCAT satellite data in the summer monsoon pattern (Fig. 2a). In October and November, the monsoon trough moves to the southern part of the SCS, which is consistent with the positive mean RVSW in the southern part of the SCS in the winter monsoon pattern (Fig. 2b).

Another reason for the formation of the positive and negative vorticity in the SCS is the coastal mountains around the SCS (Fig. 5). Xie et al. (2003) showed that the positive wind stress curl in the northern SCS in summer is due to Annam Cordillera, a north-to-south mountain range on the east coast of the Indochina Peninsula. As the summer southwest monsoonal winds impinge on Annam Cordillera, the orographic blockage accelerates the winds on the southern tip of Annam Cordillera, leading to the formation of a strong wind jet offshore (Fig. 1a). The increased wind speed due to this wind jet causes the positive RVSW in the northern part of the SCS and the negative RVSW in the

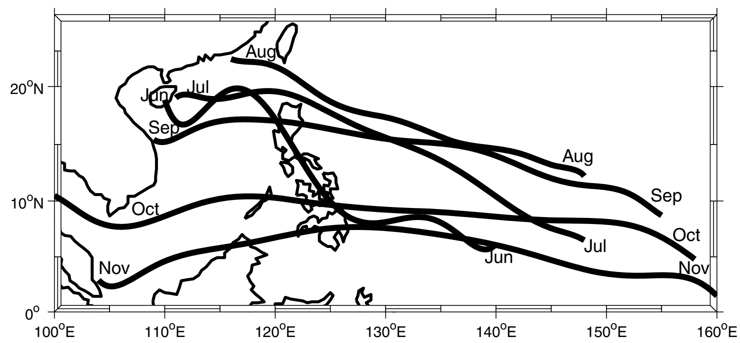

Fig. 3. Typical migration of the axis of the monsoon trough indicated by its mean monthly positions from June to November. The mean monthly positions are derived from the seven-year mean wind field from QuikSCAT measurements (from July 1999 to June 2006) by determining the interface of the monsoon westerlies and the trade easterlies.

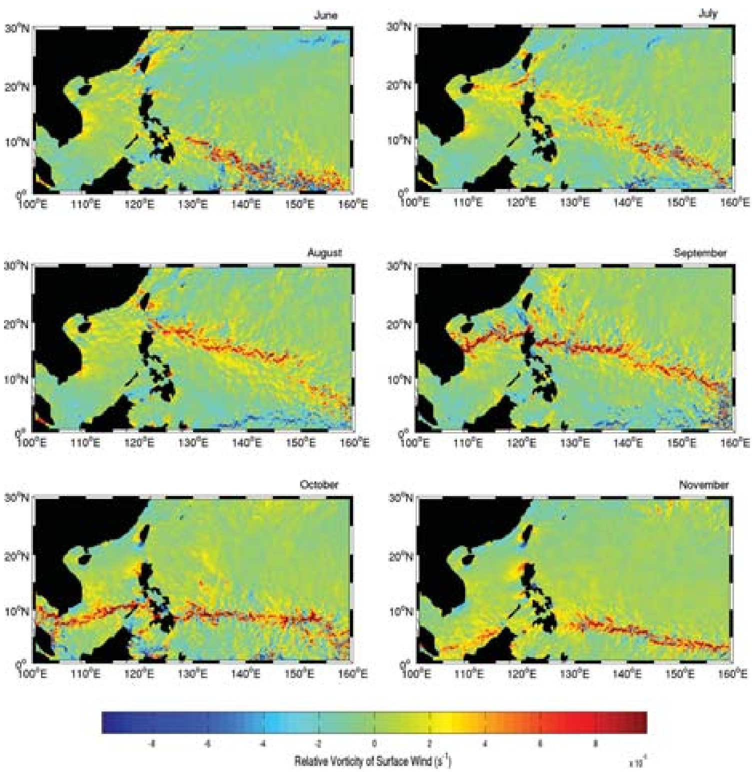

Fig. 4. The mean RVSW from June to November derived from seven-year QuikSCAT satellite data (from July 1999 to June 2006). The monsoon trough can be observed clearly as the zone with high positive RVSW.

southern part of the SCS (Fig. 2a) during the summer monsoon. In the winter monsoon months, there is a northeast-to-southwest oriented jet stream across the Luzon Strait (Fig. 1b). Similar to the summer monsoon conditions, this jet stream is caused by the coastal mountains in Taiwan and Luzon Island. The increased wind speed due to this wind jet in the winter monsoon months leads to the negative RVSW in the northern part of the SCS and the positive RVSW in the southern part of the SCS (Fig. 2b).

Previous studies have revealed that about 80% of TCs form in the monsoon trough in the WNP (including the SCS), and the remainder form from waves in the easterlies, in conjunction with upper cold lows, or in the baroclinic zones of intruding mid-latitude troughs (McBride, 1995). Ritchie and Holland (1999) identified five characteristic patterns associated with TC genesis in the WNP: monsoon shear line, monsoon confluence region, monsoon gyre, easterly waves and Rossby energy dispersion. The relationship between the mean position of the monsoon trough and the mean TC genesis location is apparent in the WNP, but the monthly mean TC genesis location tends to lag the north-to-south shift of monsoon trough by a few degrees of latitude (Chia and Ropelewski, 2002), one possible reason for which is that not all TCs form in the monsoon trough. Comparing Fig. 3 and Fig. 5, the monthly mean TC genesis location in the SCS also tends to lag the north-to-south shift of monsoon trough by a few degrees of latitude, which is similar to the characteristics of cyclogenesis in the WNP.

As a semi-enclosed marginal sea under significant influences of the monsoon, the SCS shows some unique climatic characteristics that differ from those seen in the open ocean. As seen

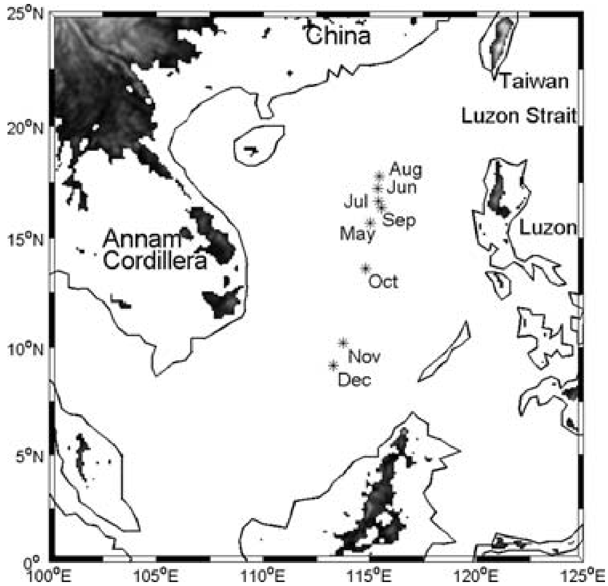

Fig. 5. Monthly mean TC genesis position from 1945 to 2005 in the SCS. The mean geneses positions are indicated by asterisks and the corresponding months are indicated near the asterisks. Land topography with elevations greater than 500 m is shaded. The Annam Cordillera is a north-south running mountain range on the east coast of Indochina Peninsula.

in Fig. 3, the monsoon trough shifts more northward during the summer monsoon compared with that in the NWP, which suggests a stronger influence of the summer monsoon in the SCS. Under the significant influences of the monsoon, the distribution of the mean RVSW and the TC genesis locations can be classified into two patterns, the summer monsoon pattern and the winter monsoon pattern. The SCS is surrounded by several coastal mountains (Fig. 5), which is a feature that differentiates it from the open ocean (e.g. WNP). The RVSW induced by these coastal mountains also affects the TC formation in the SCS. The timing of the positive mean RVSW induced by the coastal mountains coincides with increased mean RVSW caused by the annual movement of the monsoon trough. This combination of interconnected climatic patterns leads to a pre-disposition for TC development in the northern SCS during the summer monsoon season and in the southern SCS during the winter monsoon season. For regions with negative RVSW induced by coastal mountains (the region south of 10 °N during the summer monsoon and the northernmost region during the winter monsoon), although the monsoon trough does not exist in these regions, other factors (e.g. easterly waves and baroclinic disturbances) could possibly trigger cyclogenesis. However, almost no TCs were formed in these regions with negative RVSW during either summer or winter monsoons in the past 61 yr (1945–2005), which suggests that the mean negative RVSW induced by coastal mountains can prohibit TC formation.

4. The RVSW prior to TC genesis in the SCS

Section 3 associates the seven-year mean RVSW, representing the background conditions of RVSW, with TC genesis in the SCS. While these background conditions play an important role in providing a foundation for TC formation, it is synoptic-scale waves/disturbances that often serve as perturbations for triggering individual cyclogenesis events (Li et al., 2003). Recent satellite products provide a great opportunity to reveal synoptic-scale wave structures prior to TC formation, for example in the study of Li et al. (2003) synoptic wave structures prior to cyclogenesis due to Rossby wave energy dispersion and the easterly wave forcing mechanism were revealed from direct QuikSCAT satellite measurements.

In the following, the RVSW due to synoptic-scale waves/disturbances prior to TC genesis is investigated. In all, 36 TCs formed in the SCS from July 1999 to June 2006, during which time QuikSCAT measurements are available. The mean RVSW was calculated for the 3 d immediately prior to the genesis of these 36 TCs using QuikSCAT measurements. Considering that TCs have areas of positive near-surface vorticity ranging in size from 100 to 1000 km (Liu and Chan, 1999), we firstly determined the calculated area of mean RVSW for each individual TC. The three-day mean RVSW was calculated in regions around the TC genesis locations with a radius from 50 km to 500 km with 50 km increments, and then the radius with the maximum mean RVSW among all radii was chosen to calculate the area. The calculated three-day mean RVSW and seven-year monthly mean RVSW for the determined area, with the addition of the planetary vorticity at the TC genesis position for these 36 TCs are presented in Fig. 6. On average, the three-day mean RVSW in the chosen calculated area before TC genesis is 6.19×10^{-5} s^{-1} with a standard deviation of 4.79×10^{-5} s^{-1}, which is about 1.7 times the mean planetary vorticity (3.63×10^{-5} s^{-1}) and about 5.0 times the seven-year monthly mean RVSW (1.25×10^{-5} s^{-1}). The calculated value of the three-day mean RVSW before TC genesis (6.19×10^{-5} s^{-1}) is greater than the criteria for Atlantic TC genesis with relative vorticity (4×10^{-5} s^{-1}) at 700 hpa determined by the National Centers for Environmental Prediction (NCEP) global model (DeMaria et al., 2001). The mean absolute vorticity (the mean RVSW plus the planetary vorticity) of these 36 TCs is 9.83×10^{-5} s^{-1}, with a standard deviation of 5.09×10^{-5} s^{-1}.

5. Discussion and conclusion

The effects of the seven-year mean RVSW representing the background conditions and the three-day mean RVSW prior to TC genesis representing the synoptic-scale perturbations on the TC genesis in the SCS, a typical semi-enclosed marginal sea under significant influences of the monsoon, are investigated using the QuikSCAT satellite measurements.

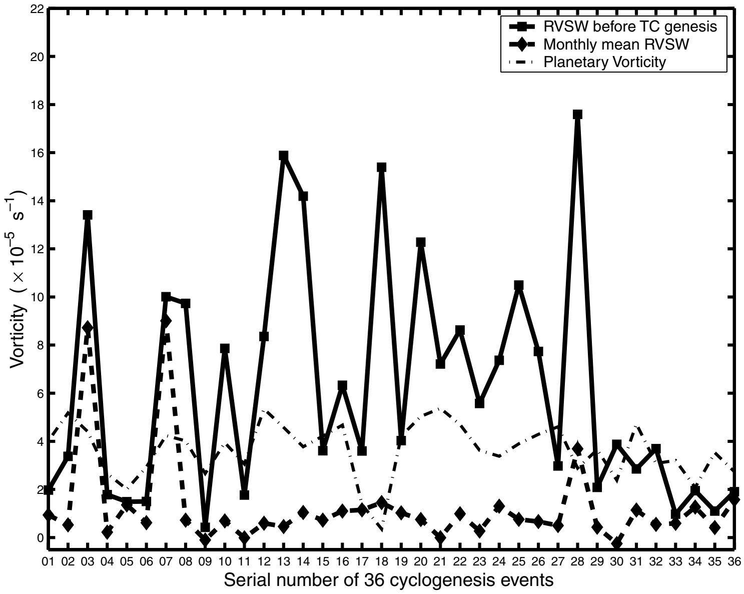

Fig. 6. The calculated three-day mean RVSW before TC genesis and seven-year monthly mean RVSW in the determined calculated area around the TC genesis position, with the addition of the planetary vorticity at the TC genesis position for 36 cyclogenesis events in the SCS from July 1999 to June 2006.

A relationship between the distribution of the seven-year mean RVSW and genesis locations of TCs in the SCS is revealed. During the summer monsoon season, TCs are formed in the northern SCS, where monsoon trough and coastal mountains contribute to positive mean RVSW, while in the winter monsoon period TCs form in the southern SCS with positive mean RVSW. No TCs formed in the southern part of the SCS during the summer monsoon nor in the northern part during the winter monsoon throughout the period from 1945 to 2005, both of which coincide with negative mean RVSW induced by the coastal mountains. Wang et al. (2007) revealed that no TCs originated from the region south of 10 °N during summer monsoon months in the past 61 yr (1945–2005), although necessary oceanic thermodynamic conditions existed in this region during summer monsoon months. From the present study, we found that negative RVSW induced by coastal mountains is a factor that inhibits TC formation in this region.

The RVSW characteristics prior to TC formation were studied using three-day QuikSCAT data immediately prior to the genesis of 36 TCs formed in the SCS from July 1999 to June 2006. The three-day mean RVSW in regions around the TC genesis locations in these 36 cyclogenesis events is 6.19×10^{-5} s^{-1}, which is about 1.7 times the planetary vorticity and about 5.0 times the seven-year monthly mean RVSW in the same region. According to quantitative calculations for these 36 cyclogenesis events, the synoptic-scale waves/disturbances prior to TC formation, which trigger the cyclogenesis, tend to increase the RVSW to be about five times the background mean RVSW. The results of these quantitative calculations using the direct QuikSCAT satellite observations support the hypothesis given by Gray (1975) that above-normal low-level relative vorticity is necessary for the occurrence of tropical cyclogenesis.

6. Acknowledgments

The authors are grateful to Remote Sensing Systems for providing the QuikSCAT satellite data and the Joint Typhoon Warning Center (JTWC) for the best-track data. This work was supported by RGC grant NSFC/HKUST36, RGC 402103, UGC under grant no. HIA02/03.SC04, N_HKUST630/04 and NSFC Grant no.49910161986. The authors thank two thorough and helpful anonymous reviewers for their comments and suggestions.

References

Bliven, L. F., Branger, H., Sobieski, P. W. and Giovanageli, J. P. 1993. An analysis of scatterometer returns from a water agitated by artificial rain. *Int. J. Remote Sens.* **14**, 2315–2329.

Chelton, D. B., Schlax, M. G., Freilich, M. H. and Milliff, R. F. 2004. Satellite measurements reveal persistent small-scale features in ocean winds. *Science* **303**, 978–983.

Chen, L. S. and Ding, Y. H. 1979. *An Introduction to the West Pacific Ocean Typhoons*. Science Press, Beijing, China, p. 400–490 (In Chinese).

Chen, T.-C., Weng, S. P., Yamazaki, N. and Kiehne, S. 1998. Interannual variation in the tropical cyclone formation over the western North Pacific. *Mon. Wea. Rev.* **126**, 1080–1090.

Chia, H. H. and Ropelewski, C. F. 2002. The interannual variability in the genesis location of tropical cyclones in the Northwest Pacific. *J. Clim.* **15**, 2934–2944.

DeMaria, M., Knaff, J. A. and Connell, B. H. 2001. A tropical cyclone genesis parameter for the tropical Atlantic. *Wea. Forcasting* **16**, 219–233.

Freilich, M. H. and Dunbar, R. S. 1999. The accuracy of the NSCAT-1 vector winds: comparisons with NDBC buoys. *J. Geophys. Res.* **104**, 11,231–11,246.

Gray, W. M. 1968. Global view of the origin of tropical disturbances and storms. *Mon. Wea. Rev.* **96**, 669–700.

Gray, W. M. 1975. Tropical cyclone genesis. Atmospheric Science Paper 234, 121 pp. [Available from Dept. of Atmos. Sci., Colorado State University, Fort Collins, CO 80523.]

Katsaros, K. B., Forde, E. B., Chang, P. and Liu, W. T. 2001. QuikSCAT's SeaWinds facilitates early identification of tropical depressions in 1999 hurricane season. *Geophys. Res. Lett.* **28**, 1043–1046.

Lau, K. H., Zhang, Z. F., Lam, H. Y. and Chen, S. J. 2003. Numerical simulation of a South China Sea typhoon Leo (1999). *Meteorol. Atmos. Phys.* **83**, 147–161.

Li, T., Fu, B., Ge, X., Wang, B. and Peng, M. 2003. Satellite data analysis and numerical simulation of tropical cyclone formation. *Geophys. Res. Lett.* **30**, 2122, doi: 10.1029/2003GL018556.

Liang, B. Q. 1991. *Tropical atmospheric circulation system over the South China Sea*. China Meteorology Press, Beijing, China, p. 100–224 (in Chinese).

Liu, K. S. and Chan, J. C. L. 1999. Size of tropical cyclones as inferred from *ERS-1* and *ERS-2* data. *Mon. Wea. Rev.* **127**, 2992–3001.

McBride, J. L. 1981. Observational analysis of tropical cyclone formation. Part I: Basic definition of data sets. *J. Atmos. Sci.* **38**, 1117–1131.

McBride, J. L. 1995. Tropical cyclone formation. Chap.3, Global perspectives on tropical cyclones. Tech. Doc. WMO/TD No. 693, World meteorological organization, Geneva, Switzerland, 63–105.

Ritchie, E. A. and Holland, G. J. 1999. Large-scale patterns associated with tropical cyclogenesis in the western Pacific. *Mon. Wea. Rev.* **127**, 2027–2043.

Sharp, R. J., Bourassa, M. A. and O'Brien, J. J. 2002. Early detection of tropical cyclones using seawinds-derived vorticity. *Bull. Amer. Meteor. Soc.* **83**, 879–889.

Sobieski, P., Craeye, C. and Bliven, L. F. 1999. Scatterometric signatures of multivariate drop impacts on fresh and salt water surfaces. *Int. J. Remote Sens.* **20**, 2149–2166.

Wang, L., Fung, C. H. and Lau, K. H. 2007. The upper ocean thermal structure and the genesis locations of tropical cyclones in the South China Sea. *J Ocean University of China*, **6**, 125–131.

Wang, Z. L. and Fei, L. 1987. *Manual for Typhoon Prediction*. China Meteorology Press, Beijing, China, 260–287 (In Chinese).

Weissman, D. E., Bourassa, M. A. and Tongue, J. 2002. Effects of rain rate and wind magnitude on SeaWinds scatterometer wind speed errors. *J. Atmos. Oceanic Technol.* **19**, 738–746.

Wu, D. S., Zhao, X., Feng, W. Z. and Ma, Y. 2005. The statistical analyses to the local harmful typhoon of South China Sea. *J. Tropic. Meteor.* **21**, 309–314 (In Chinese).

Wyrtki, K. 1961. Scientific results of marine investigations of the South China Sea and Gulf of Thailand 1959–1961. NAGA Rep.2, 50–195, Scripps Inst. of Oceanogr., La Jolla, Calif.

Xie, S. P., Xie, Q., Wang, D. X. and Liu, W. T. 2003. Summer upwelling in the South China Sea and its role in regional climate variations. *J. Geophys. Res*. **108**(C8), 3261, doi: 10.1029/2003JC001867, 17–1 – 17–13.

Zhang, X. Y. and Lin, X. G. 2001. Some statistical features of tropical cyclones originating from northeast South China Sea. *J. Tropic. Oceanogr.* **20**, 61–67 (In Chinese).

Zhang, Z. F. 2003. *Study of South China Sea typhoons between 1999 and 2002*. PhD thesis, Hong Kong University of Science and Technology, 50–83.